Delocalized Bonding

DOI: 10.1002/anie.200804397

Delocalized Metal–Metal and Metal–Ligand Multiple Bonding in a Linear Ru−Ru≡N Unit: Elongation of a Traditionally Short Ru≡N Bond**

*József S. Pap, Serena DeBeer George, and John F. Berry**

Binuclear metal–metal bonded complexes such as $[Rh_2(OAc)_4]$ (Scheme 1, **A**) are celebrated because of their unmatched ability to catalyze reactions that directly functionalize C−H bonds.[1] These metal–metal bonded catalysts function by assisting the transfer of a carbene or nitrene group (CR_2 or NR, respectively) to an organic substrate.[1] The key intermediates in these C−H activation reactions are proposed to have structures such as **B** (Scheme 1) that feature both a metal–metal bond and a metal–ligand multiple bond. Despite many years of mechanistic study on these reactions, no multiply bonded species, such as **B**, has, to our knowledge, ever been isolated and characterized.[2] In order to synthesize an M−M≡E metal–metal/metal–ligand multiply bonded system, we chose to target a Ru−Ru≡N nitrido complex (Scheme 1, **C**) for which no structural precedents exist. This species could be synthesized from thermal or photolytic decomposition of the appropriate Ru−Ru−N_3 azido precursor.[3] This experimental strategy is attractive because synthetically useful $[Ru_2(L)_4X]$ compounds (L = ligand) are well known[4] and also because Ru is known to stabilize mononuclear nitrido Ru^{VI} complexes[5] that form a useful comparison to **C**.

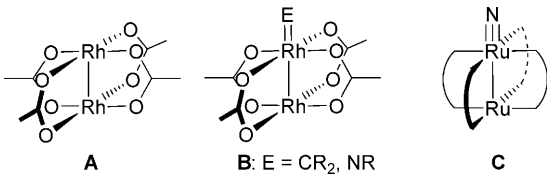

Scheme 1. Structure of $[Rh_2(OAc)_4]$ catalyst (**A**), the proposed multiply bonded intermediate (**B**), and the proposed diruthenium model compound (**C**).

We used the previously reported azido compound $[Ru_2(dPhf)_4N_3]$ (**2**, dPhf = *N*,*N*′-diphenylformamidinate)[6] as a precursor for the photoreaction (Scheme 2), since it has intense absorption bands at 520 nm and 660 nm.[6] The nitrido complex, $[Ru_2(dPhf)_4N]$ (**1**) was detected in positive-ion mode MALDI-TOF experiments on **2**. At low laser power, only one set of peaks with the characteristic distribution of natural Ru isotopes can be seen, centered at 984.1, which is assigned as $[\mathbf{2}-N_3]^+$ whereas, at higher laser power, a new set of peaks is detected at 14 mass units higher (998.1), that is ascribed unequivocally to $\mathbf{1}^+$, as is further supported by the calculated isotopic pattern.[7]

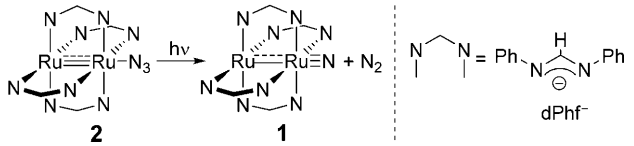

Scheme 2. Synthesis of nitrido complex **1** from azido complex **2**.

Owing to its quartet ground state, the X-band EPR spectrum of **2** at 8 K features a distinct $S = 3/2$ signal at $g_{eff} = 4.22$. Photolysis of **2** at −40 °C produces a new sharp axial $S = 1/2$ EPR signal, described below, that is unmistakably due to a highly reactive intermediate species because it decays rapidly at −40 °C.

Photolysis of frozen samples of **2** in CH_2Cl_2 at 77 K allowed us to maximize the yield of this new species, and to observe an accompanying color change from purple to pink upon its formation (UV/Vis spectroscopic data are given in the Supporting Information). The new axial EPR signal (Figure 1) clearly indicates an $S = 1/2$ species that we suggest is due to the photooxidation product $[Ru_2(dPhf)_4N]$ (**1**), because photooxidation formally removes two electrons from the $\{Ru_2\}$ moiety, leaving only one unpaired electron located in an Ru_2 δ* orbital (see below). Simulation of the EPR data yielded *g* tensor components, $g_\perp = 2.189$ and $g_\parallel = 1.900$, consistent with axial molecular symmetry. The $g_\parallel$ value < 2.00 suggests spin-orbit coupling with vacant d-orbital-based molecular orbitals, that is, a higher oxidation state for the diruthenium core. Introduction of hyperfine coupling to ^{101}Ru and ^{99}Ru nuclei (both have $I = 5/2$ with 17% and 12.8% natural abundance, respectively) that are statistically distributed between two non-identical Ru positions was also necessary for an accurate simulation. The hyperfine couplings

[*] Dr. J. S. Pap, Dr. J. F. Berry
Department of Chemistry, University of Wisconsin
1101 University Ave., Madison, WI 53706 (USA)
Fax: (+1) 608-262-6143
E-mail: berry@chem.wisc.edu
Dr. S. DeBeer George
Stanford Synchrotron Radiation Lightsource, SLAC
Stanford University, Stanford, CA 94309 (USA)

[**] We are grateful to the University of Wisconsin for providing generous startup funds. We also thank Prof. Thomas Brunold for access to the resonance Raman facility, and Michael Nippe for assistance with the mass spectrometry. SSRL operations are funded by DOE, BES. The SMB program is supported by NIH, NCRR, BMTP and by DOE, BER.

Supporting information for this article is available on the WWW under http://dx.doi.org/10.1002/anie.200804397.

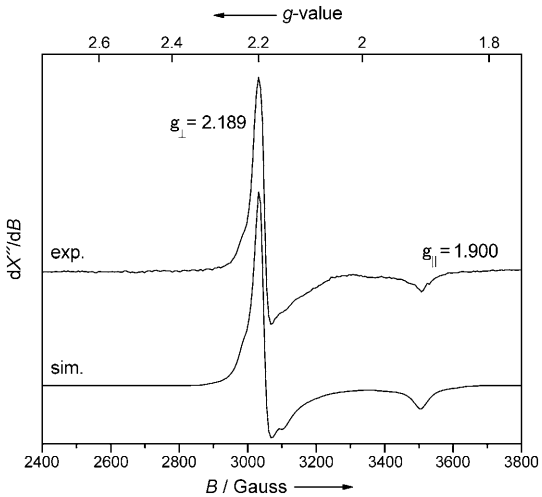

Figure 1. X-band EPR spectrum of **1** (110 K) and a simulated spectrum below.

(A) between the unpaired electron and the nuclear magnetic momenta of the two nonequivalent ruthenium nuclei differ significantly ($A_{\perp}^{Ru1} = 20 \times 10^{-4}\,cm^{-1}$ and $A_{\parallel}^{Ru1} = 35 \times 10^{-4}\,cm^{-1}$; $A_{\perp}^{Ru2} = 6 \times 10^{-4}\,cm^{-1}$ and $A_{\parallel}^{Ru2} = 11 \times 10^{-4}\,cm^{-1}$) though both hyperfine tensors are axially symmetric, in agreement with the molecular geometry of **1**.

The resonance Raman (RR) spectrum of a photolyzed sample of **2** was measured (Figure 2). A striking feature of the spectrum is that the azide stretching band at 2058 cm^{-1} that dominates the IR spectrum of **2** is missing, consistent with photochemical generation of **1**. Additionally, a new group of overlapping bands appears with the highest intensity signal at 847.2 cm^{-1}, which is not present in the IR spectrum of **2**.[7] An isotopically substituted derivative of **2** was also prepared, **^{15}N-2**, that bears a ^{15}N-labeled azido ligand (^{15}N-^{14}N-^{14}N) that may bind to ruthenium at either the ^{15}N or the ^{14}N atom with equal probability. Photolysis of **^{15}N-2** produces a mixture of **1** and **^{15}N-1**, the RR spectrum of which shows an isotopic shift of the band at 847.2 cm^{-1} to 822.6 cm^{-1} (Figure 2). Notably, there are no other isotopically sensitive bands in the spectrum. This change of 24.6 cm^{-1} is almost exactly as predicted for the isotopic shift of an Ru≡N stretch, ν(Ru≡N), by reduced mass analysis (ν(Ru≡N) = 25.1 cm^{-1}). We therefore assign the band at 847.2 cm^{-1} as ν(Ru≡N) for **1**. Irradiation of a KBr pellet containing **2** resulted in similar changes in the IR spectrum.[7] In this case, ν(Ru≡N), found at 851.5 cm^{-1} in the room temperature IR spectrum, is both Raman and IR active as expected for a band of a_1 symmetry in the C_{4v} point group.

It is useful to compare the ν(Ru≡N) value of **1** to those of previously characterized mononuclear Ru^{VI} nitrido compounds,[5] as the stretching frequency is an indicator of bond strength. The ν(Ru≡N) frequencies in Ru^{VI}–nitrido compounds vary between 1000 and 1100 cm^{-1} as seen in Figure 2, and reflect an Ru≡N bond order of 3 (one σ and two π bonding MOs, formed by overlap of the filled N 2p orbitals and the empty ruthenium d_{z^2}, d_{xz} and d_{yz}). We may also compare the value of ν(Ru≡N) in **1** to the Ru≡N stretching frequencies for nitrogen atoms bound at Ru(0001) ($\nu_{\perp}$(Ru≡N) 573 cm^{-1})[8a,b] and Ru(10$\bar{1}$0) ($\nu_{\perp}$(Ru≡N) 484 cm^{-1})[8c]

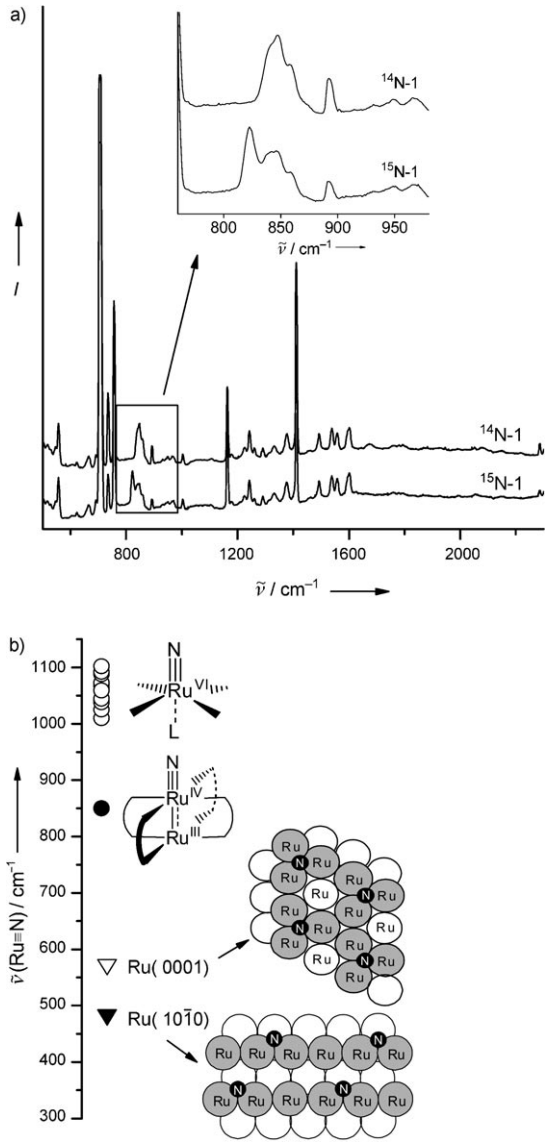

Figure 2. a) Resonance Raman spectra of **1** and **^{15}N-1** measured at 77 K with an excitation wavelength of 514.5 nm. b) Comparison of Ru–N stretching frequencies for mononuclear Ru^{VI}–nitrido complexes ○, N-atoms attached to Ru single-crystal surfaces ($\nu_{\perp}$ modes) ▽ and ▼, and **1** ●.

surfaces, which represent key intermediates in ammonia synthesis by the Haber-Bosch process. These stretching frequencies are much lower than those of the mononuclear complexes, or of **1**, which is partly due to a weaker bonding interaction, and partly due to the nitrogen atoms bridging three neighboring Ru atoms. The long Ru–N bond length (1.93 Å on Ru(0001) surfaces)[8a] is in accordance with weak, but significant bonding. An important aspect of this bonding structure is that the N 2p orbitals interact with the d_{z^2} orbitals of three surface Ru atoms, raising the Ru_3N antibonding combination above the Fermi energy, thus remaining unoccupied.[8a,9] Thus the delocalized energy levels of the bulk ruthenium atoms act as a buffer for electrons that would destabilize the Ru≡N bond. The new Ru–Ru≡N species **1**, in this respect, lies between the extremes of a mononuclear

Ru^{VI}–nitrido and a Ru-surface-bound nitrogen atom, indicative of a new type of metal–nitrogen interaction.

Owing to the instability of **1** in solution, it has thus far been impossible to obtain this species in crystalline form. We have therefore accessed structural information for **1** from X-ray absorption (XAS) data. Figure 3 shows Ru K-edge XAS

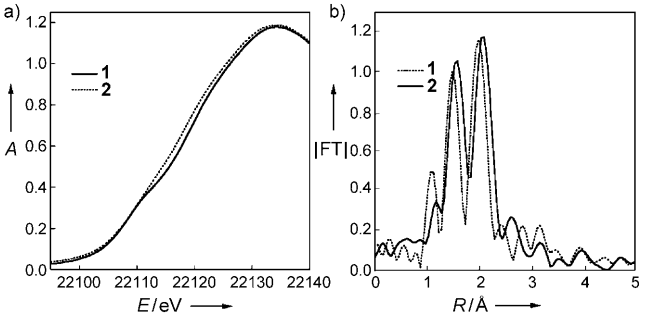

Figure 3. a) Comparison of the normalized Ru K-edge data for **1** and **2**. b) The non-phase shift corrected Fourier transforms for **1** and **2**.

data for frozen solutions of **2** before and after irradiation, for which approximately 85% conversion into **1** was confirmed by EPR spectroscopy. The edge region for **2**, which is similar to that measured separately for a polycrystalline sample of **2**, is broad and featureless, with a major inflection at 22116.5 eV. The edge energy for **1**, 22117.9 eV, is approximately 1 eV higher than that for **2**, signifying an increase in the formal Ru oxidation state of one unit per Ru atom. This change is consistent with the oxidation of $\{Ru_2\}^{5+}$ in **2** to the novel $\{Ru_2\}^{7+}$ core in **1**. There is also a notable pre-edge shoulder in **1** that may be attributed to p/d orbital mixing in the virtual orbital levels, mediated by the Ru–N σ interaction. Alternatively, this feature could be due to a 1s-to-5p ligand-to-metal charge-transfer transition, which gains intensity as a result of the covalent Ru–nitrido interaction.

The EXAFS region of the spectrum was also analyzed so that Ru–ligand bond lengths could be ascertained. The data for **2** in frozen CH_2Cl_2 solution are similar to those obtained for the solid sample. More importantly, data for both of these samples could be fitted with structural parameters (4.5 Ru–N vectors of 2.06 Å, and one Ru–Ru vector of 2.33 Å) that are consistent with the crystal structure of **2** (Ru–N bond lengths of 2.06-2.08 Å and a Ru–Ru bond length of 2.34 Å).[6] The EXAFS spectroscopic data for **1** are significantly different from those of **2** and could not be fitted without the inclusion of a short Ru–N vector of 1.76 Å that we propose is due to the Ru≡N group. Whereas the other Ru–N bond lengths in **1** remain at 2.07 Å, the Ru–Ru bond length of 2.42 Å is significantly lengthened by approximately 0.09 Å in comparison to **2**, signifying a loss of metal–metal multiple bonding. The Ru≡N bond in **1** is also significantly longer, by 0.16 Å, than Ru≡N bond lengths in mononuclear Ru^{VI}–nitrido species.[5] The only terminal Ru≡N bond length comparable to that of **1** is found in a Ru^{V}–nitrido species (ca. 1.74 Å),[10] in which one of the three d electrons from the Ru^{V} center occupies a Ru–N π* antibonding orbital, which leads to a lower bond order and corresponding elongation of the Ru≡N bond.

Density functional theory (DFT) was used to calculate the electronic structure of $[Ru_2(HNCHNH)_4N]$, **1mod**, a model for **1** in which the eight phenyl rings have been replaced by hydrogen atoms to facilitate computations. The structure of **1mod** converged to a minimum-energy geometry with bond lengths of 2.51 Å for Ru–Ru and 1.72 Å for Ru≡N that are in reasonable agreement with those found for **1** by EXAFS spectroscopy. Other properties of **1mod** that have been calculated include the vibrational frequencies. The Ru–Ru stretching frequency, which, although it was not experimentally detected, is calculated to appear at 230 cm^{-1}. The calculated ν(Ru≡N) value, 882 cm^{-1}, is in good agreement with the experimentally determined value, 848 cm^{-1}. The g tensor for **1mod** was also calculated, $g_{\|} = 1.92$ and $g_{\perp} = 2.62$, and was found to be in good qualitative agreement with the experimental EPR spectrum in that both the experimental and computed g tensors are axial with $g_{\|} < 2.00$. The computed $g_{\perp}$ value is significantly different from that observed by EPR ($g_{\perp} = 2.19$), as is to be expected because the orbital containing the unpaired electron has Ru_2 δ* character and also has a major contribution from the equatorial ligand ($HNCHNH^-$ in the case of **1mod**, but $dPhf^-$ in the case of **1**).

The electronic structure of **1mod** is unique. The terminal N atom adds a major perturbation to the typical ordering of the Ru_2 orbitals (σ, 2π, δ, δ*, 2π*, σ*)[4] by interacting strongly with the σ and π orbitals. The Ru_2 orbitals of δ symmetry are unchanged, but three-center Ru–Ru≡N orbitals are formed for both the σ and π sets. The resulting three-center orbitals (Figure 4) consist of bonding, nonbonding (n.b.), and antibonding (*) combinations of the σ orbitals (formed from the overlap of the Ru d_{z^2} orbitals and the N p_z orbital) and π orbitals (formed from the Ru d_{xz} and d_{yz} orbitals overlapping with the N p_x and p_y orbitals, respectively). Filling the orbital manifold with the nine electrons from the $\{Ru_2\}^{7+}$ group as well as six electrons from the nitrido ligand (leaving one lone pair on the N atom) yields the following electron configuration: $\sigma^2\pi^4\delta^2\sigma(n.b.)^2\pi(n.b.)^4\delta^{*1}$. The unpaired electron is

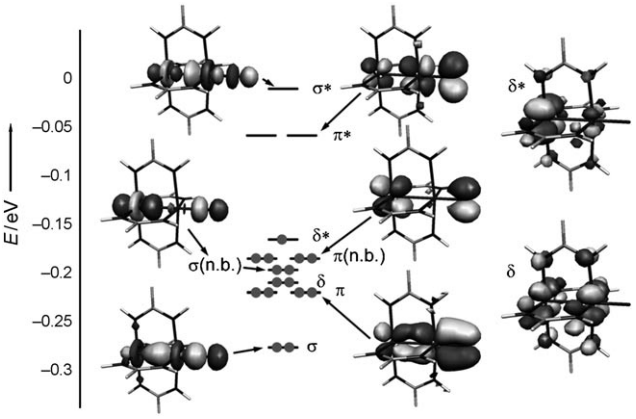

Figure 4. Molecular orbital diagram for **1mod** computed by means of DFT with contour surfaces of the three-center σ and π orbitals, δ orbitals shown to the right, and electron configuration shown as ●. n.b. = nonbonding.

thus situated in an Ru_2 δ* orbital that has no N character, and has an unsymmetrical distribution about the two Ru atoms, thus explaining the lack of ^{14}N superhyperfine interactions in the EPR spectrum as well as the two different Ru *A* tensors detected. The Ru–Ru≡N unit therefore involves a three-center four-electron (3c4e) σ bond and two orthogonal 3c4e π bonds. We propose that this delocalization of bonding throughout the Ru–Ru≡N chain causes the elongation of both the Ru–Ru and the Ru≡N bonds and is an important factor in stabilizing a nitrido species with the relatively low Ru oxidation state of +3.5, because the nonbonding Ru–Ru≡N orbitals can accommodate the electrons that would otherwise occupy Ru≡N antibonding orbitals in the case of a mononuclear Ru–nitrido species, similar to how bulk metal atoms act as an electron reservoir to Ru-surface-bound N atoms. An alternative oxidation state formulation for **1** is an $\{Ru_2\}^{7+}$ group having a localized $\{Ru^{II}–Ru^{V}\}$ electronic structure. Whereas this possibility has merit in the fact that the Ru≡N bond length in **1** (1.76 Å) is similar to that of a known Ru^{V}–nitrido species (ca. 1.74 Å),[10] DFT calculations on **1mod** suggest a delocalized system with no filled π* orbitals. Also, N hyperfine interactions are not detected in the EPR spectrum of **1** but would be expected in a genuine Ru^{V}–nitrido center.

In conclusion, for the first time we have demonstrated that a metal–metal multiply bonded complex is capable of binding a terminal ligand with multiple bonds. This complex is stabilized by electron delocalization over the second metal, which leads to nonbonding MO combinations that can accommodate the electrons that would otherwise occupy antibonding orbitals in a mononuclear species. The unprecedented electronic structure of **1** may lead us to better understand the unique ability of metal–metal-bonded compounds to facilitate carbene or nitrene insertion reactions into C–H bonds. We can suggest that, analogous to the delocalization-derived elongation of the Ru≡N moiety in **1**, carbenes and nitrenes may form weaker bonds to Rh_2 catalysts than they would in the case of a mononuclear species, thus rendering them more labile and available to react with substrates.

Experimental Section

Conversion of **2** into **1** was achieved by irradiation of frozen CH_2Cl_2 solutions (0.5–2 mM) of **2** immersed in a liquid nitrogen bath under a nitrogen atmosphere with light from either the 514.5 nm band of a Coherent I-305 Ar^+ laser (for resonance Raman samples), or 350 nm mercury vapor lamps in a Rayonet RPR-200 photochemical reactor (for EPR and XAS/EXAFS samples). Since most samples for resonance Raman spectroscopy were prepared at a different photolysis wavelength than the XAS and EPR spectroscopy samples, we prepared one resonance Raman spectroscopy sample in the photochemical reactor at 350 nm, and the resulting Raman spectrum was identical to those for samples irradiated at 514.5 nm. The best yields (80–85%, determined by EPR spectroscopy) were obtained after 8 h of continuous irradiation at 77 K in the photoreactor.

Received: September 5, 2008
Revised: October 11, 2008
Published online: November 25, 2008

Keywords: delocalized bonding · metal–metal interactions · nitrides · photooxidation · ruthenium

[1] a) H. M. L. Davies, J. R. Manning, *Nature* **2008**, *451*, 417; b) M. P. Doyle, *J. Org. Chem.* **2006**, *71*, 9253; c) D. J. Timmons, M. P. Doyle in *Multiple Bonds Between Metal Atoms*, 3rd ed. (Eds.: F. A. Cotton, C. A. Murillo, R. A. Walton), Springer, New York, **2005**; d) M. P. Doyle, T. Ren, *Prog. Inorg. Chem.* **2001**, *49*, 113; e) C. G. Espino, J. Du Bois in *Modern Rhodium Catalyzed Organic Reactions* (Ed.: P. A. Evans), Wiley-VCH, Weinheim, **2005**.

[2] A dirhodium complex with an axial N-heterocyclic carbene ligand has been described (J. P. Snyder, A. Padwa, T. Stengel, A. J. Arduengo III, A. Jockisch, H.-J. Kim, *J. Am. Chem. Soc.* **2001**, *123*, 11318), though it was determined that the Rh–C bond did not have significant multiple bond character.

[3] a) W. A. Nugent, J. M. Mayer, *Metal–Ligand Multiple Bonds*, Wiley, New York, **1988**; b) R. A. Eikey, M. M. Abu-Omar, *Coord. Chem. Rev.* **2003**, *243*, 83.

[4] P. Angaridis in *Multiple Bonds between Metal Atoms*, 3rd ed. (Eds.: F. A. Cotton, C. A. Murillo, R. A. Walton), Springer, New York, **2005**, pp. 377–430.

[5] a) S. K.-Y. Leung, J.-S. Huang, J.-L. Liang, C.-M. Che, Z.-Y. Zhou, *Angew. Chem.* **2003**, *115*, 354; *Angew. Chem. Int. Ed.* **2003**, *42*, 340; b) W.-L. Man, T.-M. Tang, T.-W. Wong, T.-C. Lan, S.-M. Peng, W.-T. Wong, *J. Am. Chem. Soc.* **2004**, *126*, 478; c) P.-M. Chan, W.-Y. Yu, C.-M. Che, K.-K. Cheung, *J. Chem. Soc. Dalton Trans.* **1998**, 3183; d) K.-L. Yip, W.-Y. Yu, P.-M. Chan, N.-Y. Zhu, C.-M. Che, *J. Chem. Soc. Dalton Trans.* **2003**, 3556; e) H.-C. Liang, P. A. Shapley, *Organometallics* **1996**, *15*, 1331.

[6] W.-Z. Chen, V. DeSilva, C. Lin, J. Abellard, D. M. Marcus, T. Ren, *J. Cluster Sci.* **2005**, *16*, 151.

[7] See the Supporting Information for further details.

[8] a) S. Schwegmann, A. P. Seitsonen, H. Dietrich, H. Bludau, H. Over, K. Jacobi, G. Ertl, *Chem. Phys. Lett.* **1997**, *264*, 680; b) H. Shi, K. Jacobi, G. Ertl, *J. Chem. Phys.* **1993**, *99*, 9248; c) H. Dietrich, K. Jacobi, G. Ertl, *J. Chem. Phys.* **1997**, *106*, 9313.

[9] R. Hoffmann, *Rev. Mod. Phys.* **1988**, *60*, 601.

[10] L. Bonomo, E. Solari, R. Scopelliti, C. Floriani, *Angew. Chem.* **2001**, *113*, 2597; *Angew. Chem. Int. Ed.* **2001**, *40*, 2529. A four coordinate Ru^{IV}-nitrido complex is also known but this species has a short (1.63 Å) Ru≡N bond, see: A. Walstrom, M. Pink, X. Yang, J. Tomaszewski, M.-H. Baik, K. G. Caulton, *J. Am. Chem. Soc.* **2005**, *127*, 5330.

